Direct electrochemical pathways for selenium reduction in aqueous solutions

Shiqiang Zou[1] and Meagan S. Mauter[1, *]

[1] Department of Civil and Environmental Engineering, Stanford University, Stanford, California 94305, USA

Mailing Address:

Yang and Yamazaki Environment and Energy (Y2E2) Building

473 Via Ortega

Stanford, CA 94305

[*]Corresponding author.

Meagan S. Mauter. Phone: (650) 725-4911; e-mail: mauter@stanford.edu

Abstract

Direct electrochemical reduction provides a novel strategy for selenium removal from complex wastewaters. While electrochemical Se(IV) reduction is thermodynamically favorable, anion structure reorganization hinders process kinetics and the phase of reduced Se(0) determines process performance. This study evaluates the thermodynamic and kinetic performance of Se(IV) removal via direct electrochemical reduction (SeDER) and proposes moderate heating to promote efficient and continuous process operation. We find that SeDER is a robust process that can handle 0.001-10 mM Se(IV) in a weakly acidic solution (pH 4-7). Se(IV) can be electrochemically removed from the aqueous phase through either a four- or six-electron pathway, with the former generating Se(0) directly attached to the electrode surface and the latter producing Se(-II) that is subsequently converted to Se(0). The four-electron pathway is a surface-limited process below 70 °C and terminates when cathode is fully covered with the insulative amorphous Se(0). We demonstrate that raising the solution temperature to 80 °C deposits Se(0) in a conductive crystalline form and enables continuous reduction on the electrode surface. In a simple batch process design, we observe Se(IV) removal rates of up to 89 mg h^{-1} m^{-2} of electrode surface area, up to 10 % Faradaic efficiency, and up to 95 % removal, though we observe moderate tradeoffs between these metrics depending on the electron pathway and the initial concentration of Se(IV). Our results suggest value in future work to enhance Faradaic efficiency via better reactor and electrode design, investigate parasitic reactions among competing ions, and select cost-effective electrodes for an economically competitive SeDER process.

Table of Contents

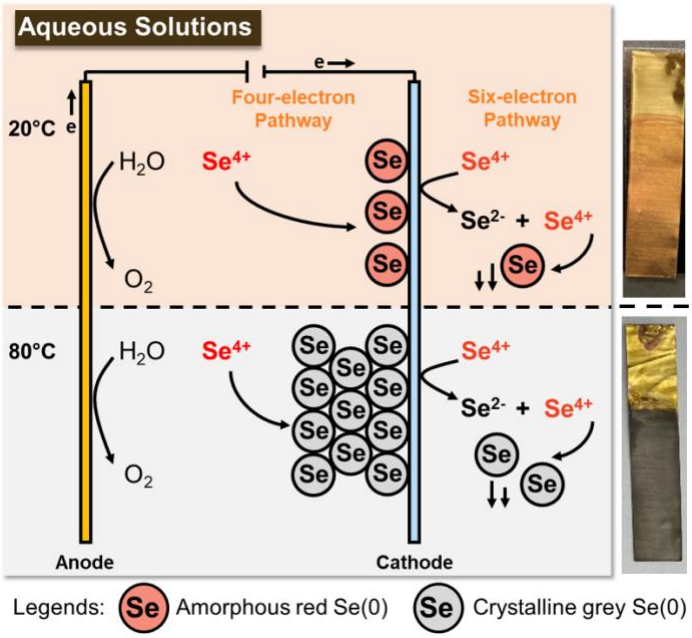

Brief Synopsis

Direct electrochemical reduction can efficiently remove Se(IV) oxyanions, providing an reliable strategy to manage Se contamination in aquatic environment.

INTRODUCTION

Selenium (Se) is a naturally occurring metalloid in earth crust that is released through natural weathering processes.[1] Anthropogenic activities have significantly accelerated geogenic release, increasing Se concentrations in aquatic environments[2] far beyond the ppb levels required for biologic function.[3] Coal-fired power plant flue-gas desulfurization (FGD) wastewater, for example, contains 1-10 mg L^{-1} Se.[4] Applications of Se-containing fertilizers coupled with water-intensive irrigation generate Se-laden agricultural drainage (100-1500 μg L^{-1}),[5, 6] and mining activities commonly discharge Se at a level of 15-50 μg L^{-1} into the aquatic environment.[7] This anthropogenic Se is primarily released as Se(IV) and Se(VI) oxyanions (e.g., SeO_3^{2-} and SeO_4^{2-}), but also includes selenocyanates ($SeCN^-$), mercury selenide (HgSe), and organic Se compounds.[8] Accumulation of Se in aquatic environments leads to bioaccumulation and ecosystem impacts, drinking water violations, and chronic health issues.[9, 10] Treatment of high-volume industrial and agricultural wastewaters is essential for complying with water quality criterion for aquatic life (1.5 and 3.1 μg L^{-1} for lentic and lotic aquatic systems)[11] and drinking water standards (50 μg L^{-1}).[12]

Conventional Se control practices use biological or physicochemical driving forces to remove Se from wastewater (Fig. 1). In biological treatment, Se-reducing bacteria either reduce Se(VI) extracellularly through a surface-displayed enzyme (e.g., gram-positive bacteria such as *B. selenatarsenatis* SF-1),[13] or assimilate Se(VI) into periplasm or cytoplasm for biomineralization (e.g., gram-negative bacteria such as *E. cloacae* SLD1a-1).[14] The generated Se(IV) is further reduced to elemental Se(0) via a microbial detoxification pathway, followed by excretion of Se(0) particles into the environment.[15] In recent years, pilot- and even full-scale bioremediation processes (e.g., ABMet®) have been commercialized to provide 99% Se removal from incoming

wastewater streams,[16] and biological Se removal is included as a "best available technology" in the U.S. EPA's Effluent Limitation Guidelines (ELGs) for the steam electric power generating category.[17] However, biological Se removal is highly sensitive to wastewater composition (e.g., sufficient carbon source, appropriate wastewater pH, few toxic substances, and low concentrations of competing oxyanions) and operation parameters (e.g., pretreatment, hydraulic retention time, and operating temperature).[6] Organic Se compounds are a frequent byproduct, and many of these compounds are significantly more bioavailable and potentially more toxic than inorganic Se.[18, 19] Finally, management of Se-rich biosolids increases the operating costs of biological processes.

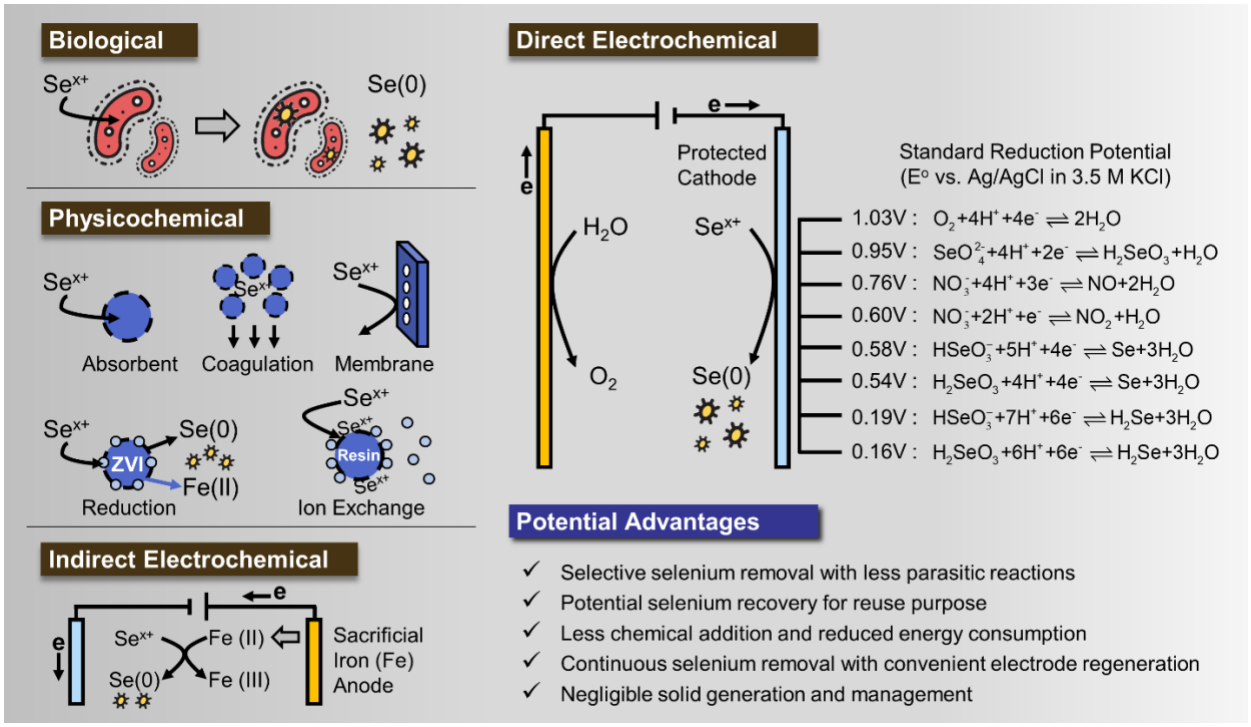

Figure 1. Comparison of existing selenium removal technologies and direct electrochemical reduction.

In contrast, physicochemical Se removal processes either rely on extensive chemical addition (e.g., Mg-Al-CO_3 sorbents, Al-based coagulants) in wastewater matrix to capture Se,[20, 21]

or pressure-driven membrane filtration to separate Se from the aqueous phase.[22] Recent work has demonstrated the efficacy of reductive reagents and anion exchange resins for chemisorbing Se oxyanions in the wastewater.[23, 24] Other work demonstrated electrosorption for environmental contaminant removal (e.g., heavy metals and Se)[25] or indirect electrochemical removal using a sacrificial iron anode to release reductive iron reagents.[26] While these physicochemical approaches are capable of providing consistent effluent quality and a reliable Se removal performance (i.e., down to the ppb level), key issues with physiochemical approaches include the generation of a large amount of solid residuals, high operational cost due to materials and solid management, elevated energy input for media regeneration, limited selectivity for Se removal in complex wastewater matrices, and mandatory system maintenance (e.g., membrane cleaning).[1, 10] In short, existing Se removal processes are energy-, resource-, and cost-intensive, driving new process development to eliminate Se oxyanions in a sustainable and economically competitive manner.

In recent years, direct electrochemical reduction (DER) has been explored for efficient ion removal (e.g., nitrate, chromate) from wastewater.[27-29] In a DER process, the cathode potential is precisely controlled to match the reduction potential of the target ions, enabling specific ion reduction in a complex water matrix (Fig. 1). DER approaches offer several advantages over indirect electrochemical reduction, including selective ion removal, fewer parasitic reactions, and reduced energy consumption. The absence of sacrificial reactions at the anode may also prolong the electrode lifespan, reduce solid production, and enable continuous process operation. DER has been extensively implemented in industrial Se plating (known as electroplating or electrodeposition) for decades on various metal surfaces, such as gold, silver, nickel, and iron.[30] Before electroplating, selenium dioxide or selenite salt is added into an acid bath (pH≤2) to prepare

the plating substrate (1-10 mM Se). The Se(IV) in the substrate is then reduced to elemental Se during electroplating, forming a thin layer of elemental Se on the target metal surface.[31, 32]

Environmental applications of Se removal via DER require mechanistic insight into the thermodynamics and kinetics of the SeDER process as a function of Se oxidation state, solution pH, Se concentration, and temperature. For example, FGD wastewater is only weakly acidic (pH=4-7) and contains comparably low levels of selenite, selenate, and other Se oxyanions (0.1-1 mM). Recently, Se removal via DER (SeDER) was performed on a strongly acidic copper refining wastewater (pH=0.3 and 3.8 mM Se) in a cyclone electrowinning reactor, and 97.6% of Se(IV) was reduced to red Se(0) within 90 mins with a faradaic efficiency of 70.6% and specific energy consumption of 0.20 kWh kg^{-1} Se.[33] To date, however, we are unaware of other efforts demonstrating SeDER from more characteristically dilute and neutral wastewater streams.

The present work evaluates the thermodynamic and kinetic performance of SeDER for environmentally relevant Se concentrations and pH ranges, while also proposing novel operational strategies for optimizing SeDER process performance under these conditions. We (1) investigate the feasibility of Se(IV)DER and Se(VI)DER in weakly acidic environments, (2) evaluate the effect of initial Se concentration and solution temperature on SeDER performance, (3) identify Se reduction pathways in simulated wastewater, and (4) quantify Se removal rate and Faradaic efficiency under long-term operation. The results from this study will inform energy-efficient and cost-effective electrochemical approaches for meeting discharge requirements in a range of industrial and agricultural wastewaters and reducing Se contamination in local ecosystems.

MATERIALS AND METHODS

Setup of the three-electrode electrochemical system. The electrochemical cells had an effective working volume of 100 mL. For each experiment, one cell served as a blank control system and was filled with 100-mL phosphate-buffered saline (PBS) solution, while the other cell was used as an experimental system and was filled with Se-spiked PBS solution. In both systems, the initial solution pH was adjusted using 1 M phosphoric acid and 1 M sodium hydroxide solution. Gold (Au) foil (Fisher Scientific, 1×5×0.125 cm, purity>99.9975%), a leakless miniature Ag/AgCl electrode (eQAD, Model ET072), and a platinum wire (CH Instrument, Model CHI 115) were used as the working electrode, reference electrode, and the counter electrode, respectively. We selected Au as the working electrode due to its excellent electrochemical stability in aqueous solutions, a wide electrochemical window, and a robust interface for oxyanion reduction and oxidative electrode cleaning. Detailed cleaning protocol of electrodes and customized 3-D printed lid design can be found in the Supporting Information (SI, Fig. S1). About 3.5 cm of the Au electrode was submerged in the solution, resulting in an effective reaction area of 7 cm^2. This three-electrode system was connected to an electrochemical potentiostat (BioLogic VSP-300) to conduct cyclic voltammetry (CV), linear sweep voltammetry (LSV), and chronoamperometry (CA). When heating was required, the electrochemical cell was placed in a sand bath on top of a magnetic stirrer hot plate to maintain a constant solution temperature. All chemicals used are purchased from Fisher Scientific and used directly without further purification (purity >99.8%). Water was from a Millipore Milli-Q system.

Experimental procedure. We first explored the feasibility of electrochemical Se reduction under weakly acidic and neutral environments. The initial solution pH was adjusted to 4.0, 5.5, and 7.0

for both control and experimental systems to simulate the pH of common industrial and agricultural wastewaters. In the experimental system, sodium selenite (Na_2SeO_3) or selenate (Na_2SeO_4) was added to maintain an initial concentration of 1-mM Se(IV) or Se(VI), respectively. Cyclic voltammetry (CV) scans were conducted in both blank control and experimental systems between -0.8 V to 1.1 V with a scan rate of 50 mV s^{-1}. Between each test, the Au electrode was electrochemically cleaned by cycling between 0.3 V and 1.5 V for ten times to fully oxidize potential residues on the electrode surface, followed by a linear sweep voltammetry (LSV) scan from 0.3 V to 1.5 V to confirm complete removal of all residues on Au electrode. Following this cleaning protocol, we fixed the pH at 5.5 for the remainder of experiments in this study. We then evaluated the effect of initial Se(IV) concentrations on SeDER performance, ranging from 0.01 mM to 10 mM Se. For each Se(IV) concentration, we performed an LSV scan towards the negative direction from 0.3 V to -0.8 V to determine the Se reduction peaks, and a follow-up LSV scan towards the positive direction from 0.0 V to 1.5 V to oxidize surface-deposited products.

To probe the mechanism of Se(IV)DER, we further utilized chronoamperometry (CA) to explore both four-electron Se(IV)/Se(0) and six-electron Se(IV)/Se(-II) reduction pathways. During each CA test, the cathode potential was held at -0.01 V, -0.25 V, or -0.61 V for 5 minutes to sustain Se(IV) reduction on the electrode surface. The initial Se(IV) level was increased to 10 mM in this test to enhance the mass transfer. After 5 minutes, we performed an LSV scan in the positive direction from 0.0 V to 1.5 V to reveal corresponding oxidation peaks of the surface-deposited reduction products. We subsequently investigated the effect of temperature on SeDER with detailed quantification of Se deposition capacity or Se deposition rate on the gold electrode under three different solution temperatures, including 20 ℃, 40 ℃, and 80 ℃. We selected a high

temperature of greater than the 50-75 ℃ range previously reported to facilitate the formation of crystalline Se(0) during electroplating processes[34] and avoid the deposition of insulative amorphous Se(0) during electrochemical reduction. A magnetic stirrer was placed inside (300 rpm) to ensure good mass transfer. As in the previous stage, the initial Se(IV) concentration was 10 mM, and each test lasted for 25 minutes.

We also performed long-term SeDER experiments with 0.001 mM (79 μg L^{-1}), 0.01 Mm (780 μg L^{-1}), and 0.1 mM (6.9 mg L^{-1}) Se(IV) to mimic Se levels common in industrial and agricultural wastewaters. Se(IV) concentration in the batch reactor was monitored to quantify Se removal rate or efficiency. Based on preliminary CV scans, the cathode was held at defined voltages corresponding to the four-electron or six-electron reduction pathway. The solution temperature was maintained under either 20 ℃ or 80 ℃. In the 6-h and 24-h tests, water samples (1 mL) were taken from the electrochemical cell every hour, and the filtered samples were preserved under 4℃ before quantification of soluble Se levels. Duplicate tests were performed in each experiment to ensure data accuracy and consistency.

Analytical methods. Current and voltage data from CV, LSV, and CA are recorded by the BioLogic potentiostat using the EC-Lab® software (BioLogic Sciences Instruments). Total soluble Se concentration in the solution is quantified by inductively coupled plasma mass spectrometry (ICP-MS). Electrodes with surface deposits were preserved in vacuum desiccators. Surface morphology and elemental mapping analysis of the gold electrodes was performed on a JEOL JXA-8230 electron probe microanalyzer (EPMA) with five wavelength dispersive X-ray spectrometers (WDS). Kinetics of electrode reactions in 0.1mM Se(IV) was performed using LSV

under various scan rates (5, 10, 20, 50, and 100 mV s^{-1}). Quantification of performance metrics, including Se removal efficiency (%), Se removal rate (mg h^{-1} m^{-2}), Se deposition capacity (mg m^{-2}), and Faradaic efficiency (%), can be found in the supporting information (SI, Eq. S1-S5).

RESULTS AND DISCUSSION

Se(IV)DER and Se(VI)DER in a weakly acidic environment. Se(IV) and Se(VI) oxyanions are the predominant species in industrial and agricultural wastewaters, with >80% of Se in its most oxidized state for some systems.[35, 36] At pH 5.5, the blank and Se(VI) CV curves are indistinguishable, but Se(IV) has distinct reduction peaks at a cathodic potential of approximately 0.0V (E vs. Ag/AgCl) and -0.6V (Fig. 2A). The second reduction peak may partially overlap with the hydrogen evolution reaction (HER) beginning at approximately -0.7V. These unique reduction peaks suggest that Se(IV) is effectively reduced on a gold electrode through two different electrochemical pathways, with generated products being subsequently oxidized under an anodic potential higher than 0.6V. We attribute the small plateau beginning at -0.1V in the blank control to the electrochemical desorption of surface-attached functional groups (e.g., Au-OH or Au-PO_4).

Theoretically, electrochemical Se(VI) reduction should be thermodynamically favorable, as indicated by the high redox potential of Se(VI)/Se(IV) couple (Eq. 1). However, the reduction of Se(VI) oxyanion to its Se(IV) counterpart is extremely slow due to the necessity of anion structure change[37] and the high activation energy required to break the Se=O double bond. While it is possible to facilitate the conversion of Se(VI) to Se(IV) using solution-phase biological or metallic catalysts,[38] doing so is not the focus of the present work.

$$SeO_4^{2-} + 4H^+ + 2e^- \leftrightarrow H_2SeO_3 + H_2O \quad E°=0.95V \text{ (E vs. Ag/AgCl)} \qquad (1)$$

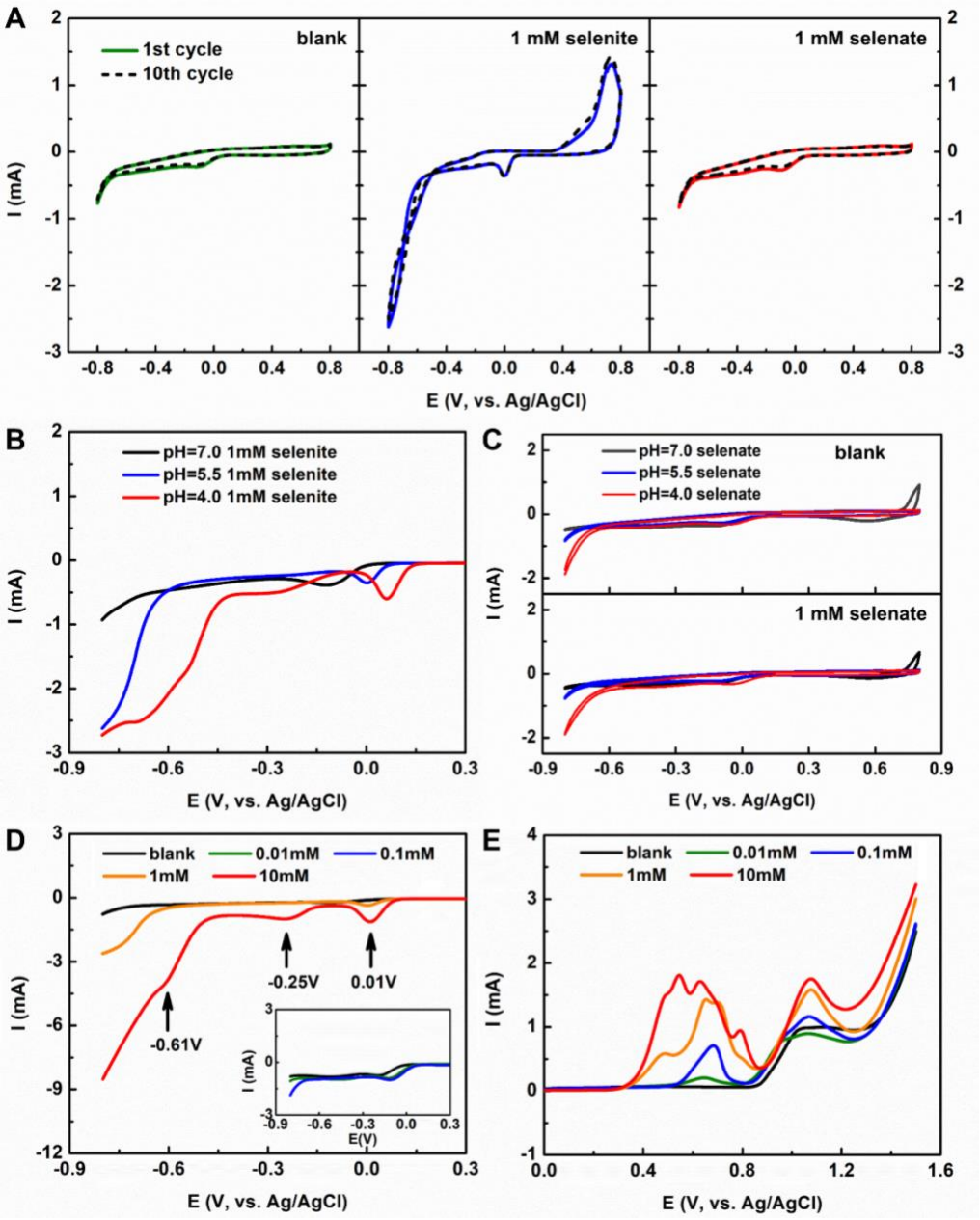

Figure 2. Direct electrochemical selenium reduction under weakly acidic environment regarding (A) CV scan for blank control, 1-mM selenite, and 1-mM selenate solution; (B) LSV of selenite reduction under three weakly acidic and neutral pH values; (C) CV scans for blank and 1-mM selenate under various pH values; (D) LSV scans under various Se(IV) concentrations in the reduction region; (E) LSV scans of the Au electrode with reduced Se(0) on the surface in the oxidation region.

We further investigated Se(IV)DER under a wider pH range of 4.0-7.0 to reflect a typical pH profile of industrial and agricultural wastewaters. In theory, solution pH affects Se(IV)DER through two pathways: (1) the elemental composition of Se oxyanions and (2) the [H^+] available for reaction. In common water matrices, the Se(IV) oxyanions are present as selenious acid (H_2SeO_3), biselenite ($HSeO_3^-$), and selenite (SeO_3^{2-}). Based on their pk_a values (Eqs. 2 and 3), we expect a comparable amount of SeO_3^{2-} and $HSeO_3^-$ at pH 7.0 and a majority of $HSeO_3^-$ at pH 5.5. Further decrease of solution pH to 4.0 would lead to a mixture of H_2SeO_3 and $HSeO_3^-$ with negligible presence of SeO_3^{2-}.

$$H_2SeO_3 \leftrightarrow HSeO_3^- + H^+ \quad pk_{a1}=2.5 \tag{2}$$

$$HSeO_3^- \leftrightarrow SeO_3^{2-} + H^+ \quad pk_{a2}=7.3 \tag{3}$$

Variation of Se(IV) composition induced by pH changes was well supported by observed reduction peaks in the LSV scan. At pH 7.0, we identified two reduction peaks for $HSeO_3^-$ (Fig. 2B), including $HSeO_3^-$/Se (E=-0.13V, Eq. 4) and $HSeO_3^-$/H_2Se (onset at -0.70V, Eq. 5). However, the absence of SeO_3^{2-} reduction peaks is a result of the significantly more negative theoretical reduction potential (Eq. 6). At pH 5.5, SeO_3^{2-} is primarily present as $HSeO_3^-$ and exhibited reduction peaks for $HSeO_3^-$/Se (0.0V) and $HSeO_3^-$/H_2Se (onset at -0.60V). In a more acidic environment (i.e., pH=4.0), H_2SeO_3 is formed in solution from $HSeO_3^-$, leading to two additional reduction peaks for H_2SeO_3/Se (E=-0.25V, Eq. 7) and H_2SeO_3/H_2Se (E=-0.70V, Eq. 8). Given the reduction potentials of these three Se(IV) species in industrial and agricultural wastewaters, the energy efficiency of Se(IV)DER may benefit from manipulating the solution pH to convert both H_2SeO_3 and SeO_3^{2-} to $HSeO_3^-$. Note that the reference E° in all equations are standard reduction

potentials measured under standard conditions (i.e., 1 M Se and 1 M H^+), and the observed E from experiment tends to be more negative due to the overpotential.

$$HSeO_3^- + 5H^+ + 4e^- \leftrightarrow Se + 3H_2O \quad E°=0.58V \text{ (E vs. Ag/AgCl)} \tag{4}$$

$$HSeO_3^- + 7H^+ + 6e^- \leftrightarrow H_2Se + 3H_2O \quad E°=0.19V \text{ (E vs. Ag/AgCl)} \tag{5}$$

$$SeO_3^{2-} + 3H_2O + 4e^- \leftrightarrow Se + 6OH^- \quad E°=-0.57V \text{ (E vs. Ag/AgCl)} \tag{6}$$

$$H_2SeO_3 + 4H^+ + 4e^- \leftrightarrow Se + 3H_2O \quad E°=0.54V \text{ (E vs. Ag/AgCl)} \tag{7}$$

$$H_2SeO_3 + 6H^+ + 6e^- \leftrightarrow H_2Se + 3H_2O \quad E°=0.16V \text{ (E vs. Ag/AgCl)} \tag{8}$$

Solution pH also alters the H^+ level in the water matrix, and high H^+ availability in an acidic water matrix would ensure a desirable reduction rate as SeDER consumes a large amount of H^+. Meanwhile, the Nernst equation dictates that Se reduction potential is strongly dependent on the $[H^+]$ in solution. For instance, assuming 1-M $HSeO_3^-$ is available in the solution, a pH increase from 0 (standard condition) to 5.5 would drop the reduction potential from 0.58V to 0.21V (273K, Eq. S6). This result was confirmed by a positive shift of the $HSeO_3^-$/Se reduction peak from -0.13V (pH=7.0) to 0.06V (pH=4.0, Fig. 2B). This positive shift in reduction peak induced by a pH decrease would require a less negatively biased cathode, which could reduce parasitic reactions on the cathode and the energy input. These conclusions align well with best practices in Se electroplating, which typically use a strong acid bath at pH 1-2 to ensure minimum energy input and high Se-film purity.[39] The obtained results indicate that we could achieve successful Se(IV)DER in a weakly acidic environment, with $HSeO_3^-$ being the preferred species for reduction. Consistent with earlier results, Se(VI)DER is a relatively inert process at pH 4-7 (Fig. 2C).

Effect of selenite concentration. In contrast to a controlled Se level in electroplating, the Se concentration in wastewater effluent is highly variable and may substantially affect SeDER. We investigated Se(IV)DER for a series of initial Se(IV) concentrations ranging from 0.01 mM to 10 mM at pH 5.5 (i.e., the average pH of FGD wastewater). Initially, a negative direction LSV scan was applied to probe electrochemical reactions in the water matrix. The Nernst equation predicts an increase in Se(VI) concentration will shift the reduction potential in the positive direction, while better mass transfer at high Se(VI) concentration is expected to enhance reduction rate and the peak heights in voltammetry. Consistent with theory, minor reduction peaks were observed for Se(IV) concentrations of 0.01mM and 0.1mM (Fig. 2D, inset), while two new Se reduction peaks emerged at 1 mM Se(IV). Based on the LSV curve of 10 mM Se (Fig. 2D), we identified three notable reduction peaks at 0.01V and -0.25V for a four-electron reduction pathway (Se(IV)/Se(0), Eq. 4), and -0.61V for a six-electron reduction pathway (Se(IV)/Se(-II), Eq. 5). Once Se(-II) is generated, a homogenous chemical reaction (Eq. 10) may yield elemental Se(0), and this chemical reaction is more favored in acidic and intermediate pH ranges.[40]

$$2H_2Se+H_2SeO_3 \leftrightarrow 3Se+3H_2O \quad (10)$$

A positive LSV scan further probed the Se reduction products on the Au electrode into the oxidation region. We identified a single oxidation peak between 0.6-0.7V (green and blue lines, Fig. 2E), revealing a Se(0) layer from underpotential deposition, though we were unable to visualize red Se films at 0.01 mM and 0.1 mM Se(IV). At Se(IV) concentrations of 1 to 10 mM, three additional oxidation peaks appeared, and visually noticeable red Se films formed on the electrode surface. These four oxidation peaks are attributed to oxidation of chemically precipitated Se(0) at 0.49 V, bulk deposited Se(0) at 0.55 V (Se-Se bond), underpotentially deposited Se(0) at

0.63 V (Se-Au bond), and subsurface Se-Au composite at 0.79V (within the Au lattice), respectively. It is also worth noting that nearly all surface deposits were oxidized during the electrochemical cleaning (procedure described in the methods), enabling convenient electrode regeneration, prolonged electrode lifespan, and reduced lifecycle treatment costs.

Four-electron vs. six-electron reduction pathway. Selecting between four- and six-electron Se reduction pathways for wastewater treatment requires a comprehensive evaluation of the tradeoffs of each approach. Within the four-electron pathway, underpotential deposition is energetically favored by Au-Se interaction and onsets at a more positive potential than that of the bulk deposition. Hence, we first evaluated SeDER through underpotential deposition and held the Au electrode at 0.01V for 5 mins. Rapid termination of underpotential deposition was observed within 10 seconds (blank line, Fig. 3A), removing a theoretical (and maximum) amount of 6.8×10^{-9} mol Se (~0.0007%) based on the current data. The reduced Se(0) would form a 160-pm layer on the Au electrode (assuming a density of 4.8 g cm^{-3}), comparable to the thickness of Se monolayer in electrodeposition on Au (200-300 pm).[41] A single oxidation peak confirmed this Se(0) layer in the positive LSV scan (green line, Fig. 3B). The results revealed that underpotential deposition is not suitable for SeDER owing to its extremely limited deposition capacity (0.77 mg m^{-2}). In subsequent tests, we held a pristine Au electrode at -0.25V for 5 mins to enable both underpotential and bulk deposition (Fig. 3C). Still, the deposited red Se(0) (i.e., the amorphous Se) with low electrical conductivity ($\sigma = 10^{-12}$ to 10^{-14} $ohm^{-1}cm^{-1}$)[42] would convert the conductive Au electrode to a nearly insulative Se electrode. We estimated that 0.005% of the Se(IV) was removed, forming a Se layer of ~1200 pm. Subsequent positive LSV scan revealed three oxidation peaks for bulk deposition (0.66 V), underpotential deposition (0.72 V), and subsurface Au-Se composite (0.82

V), respectively (blue line, Fig. 3B). The limited Se deposition capacity (5.72 mg m^{-2}) was supported by surface morphology and elemental mapping results (Fig. S2A and S2B). Hence, SeDER through a four-electron pathway (either underpotential or bulk deposition) is a surface-limited process and less competitive for continuous Se control.

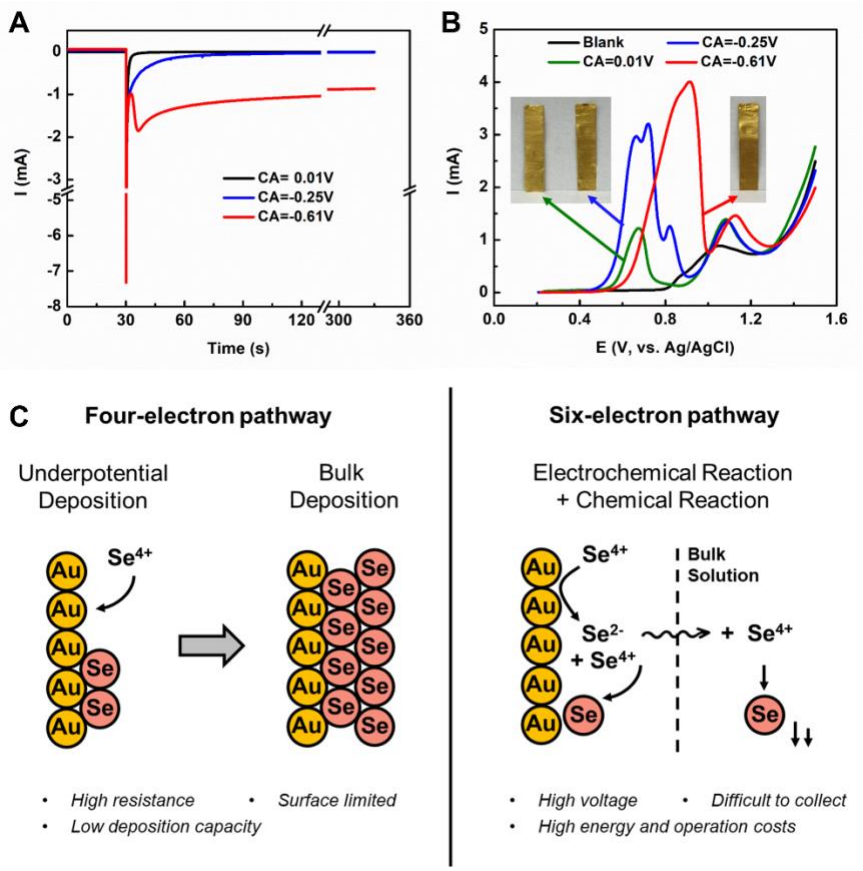

Figure 3. Electrochemical Se(IV) reduction under four-electron and six-electron pathways regarding (A) the current profile of chronoamperometry under 0.01V (underpotential deposition), -0.25V (bulk deposition), and -0.61V (six-electron reduction); (B) LSV of the Au electrode with reduced Se on the surface towards the oxidation region; and (C) schematic of four-electron and six-electron pathways with their potential application challenges.

Se(IV) reduction via the six-electron pathway generates soluble hydrogen selenide (H_2Se, aqueous) that will not cover the electrode surface, serving as a promising alternative for continuous Se removal if H_2Se could be effectively neutralized by Se(IV) in the solution phase (Eq. 10). When the Au electrode was held at -0.61 V, we observed an interesting trend of a decrease-increase-decrease current profile in duplicate tests (red line, Fig. 3A), potentially owing to a dynamic H_2Se concentration in the diffusion layer controlled by electrochemical production and consumption via chemical precipitation and physical diffusion. Note that a considerable amount of generated amorphous Se(0) was attached to the electrode surface, forming a visible red film on the Au electrode (Fig. S2C and S2D). Oxidation of the chemically precipitated Se(0) on the Au electrode revealed distinct peaks compared to that of the four-electron pathway (Fig. 4B, red line). The remaining elemental Se(0) were either suspended in the solution or settled at the bottom of the cell, requiring downstream filtration or other polishing steps to fully remove these Se particles (Fig. S3). Hence, SeDER via six-electron pathway could offer continuous Se removal, at the expense of higher exerted voltage, low Se recovery, and elevated operation cost due to downstream polishing.

When comparing four- and six-electron pathways, we need to consider the complexity of the industrial and agricultural wastewaters. These wastewaters could contain high levels of other oxyanions (up to three orders of magnitude higher than Se), such as nitrate, nitrite, phosphate, sulfate, and metal oxyanions. While not the focus of the present work, future work evaluating the respective pathways will need to perform similar experiments in the presence of competing ions relevant to the specific wastewater of interest. Nevertheless, the present results suggest that the negatively biased cathode under the six-electron pathway may promote parasitic reactions and lead to low Faradaic efficiencies. Extensive pretreatment to remove competing ions may improve the

efficiency of the six-electron pathway, but would likely come with higher capital and operational costs. In contrast, four-electron SeDER excels in system-level energy input, fewer parasitic reactions, and convenient collection of Se(0). However, to make a four-electron SeDER economically competitive, operational strategies must be proposed to tackle surface-limited reduction mechanism for significantly enhanced surface deposition capacity and Se removal efficiency.

Effect of solution temperature. Solution temperature is a vital operational parameter in SeDER that will affect not only the reaction rate but also the phase of the deposited Se(0). In this section, we investigated three solution temperatures for four-electron bulk deposition, including 20 ℃, 40 ℃, and 80 ℃. The latter two solution temperatures were selected to represent some industrial wastewaters, e.g., FGD wastewater has an average temperature of ~55 ℃.[4, 43] Under 20 ℃ and 40 ℃, the current gradually dropped to steady state at -0.020 mA and -0.037 mA (Fig. S4), respectively, over the course of the 25-min experiment. Given that the four-electron bulk deposition is a surface-limited process, these stable currents were potentially sustained by background parasitic reactions, with a faster reaction rate (and hence higher background current) at 40 ℃. We estimated the Se deposition capacity to be 8.52 mg m^{-2} at 20 ℃. The capacity was further increased to 13.25 mg m^{-2} at 40 ℃, though we could not visually identify red Se(0) films at either temperature (Fig. S5).

Further increase of solution temperature to 80 ℃ led to a relatively consistent current profile around -0.150 mA (Fig. S4). This significantly higher current indicated that we were not depositing insulative amorphous Se(0) on the electrode, but rather conductive crystalline Se(0)

with significantly higher conductivities of $\sigma = 10^{-4}$ $ohm^{-1}cm^{-1}$ at 80 °C.[44] This hypothesis was supported by visual observation of a metallic grey Se film on the electrode surface (Fig. S6) and a previous electroplating study (>55 °C).[39] Formation of crystalline Se(0) on the electrode surface effectively converts the conductive Au electrode interface to a conductive Se electrode interface, offering an innovative solution to the surface-limited four-electron reduction pathway at lower temperatures. This approach may be particularly well suited for high temperature industrial wastewater treatment where additional heat input would be minimal.

Long-term electrochemical Se removal and Faradaic efficiency. While we comprehensively investigated the operation parameters and reduction pathways of SeDER, it is of vital importance to further evaluate the extent of Se removal and the Faradaic efficiency in long-term operation. In 6-hour tests at 0.1 mM Se(IV) and 20 °C (Fig. 4A), the four-electron pathway Se(IV) concentration decreased only slightly, with removal efficiencies of 9.0 % and a Faradaic efficiency of 6.0 % (Fig. 4B). Increasing the solution temperature to 80 °C led to both an increased removal efficiency of 34.7 % and an increased Faradaic efficiency of 6.9 %. Crystalline grey Se(0) was deposited on the electrode surface, and we observed no generation of suspended or settled solids. A follow-up kinetic analysis was performed with scan rates ranging from 5 to 100 mV s^{-1} (Fig. S7 and S8). These results suggest that four-electron pathway is a quasi-reversible reaction controlled by mass transport (i.e., diffusion limited),[45] with a diffusion coefficient and standard rate constant of 6.94×10^{-5} cm^2 s^{-1} and 3.16×10^{-7} cm s^{-1} (Eq. S7-S11).[32] To conclude, Se removal via a four-electron pathway will either require a large electrode surface or extended retention times to lower the Se level in wastewaters for U.S. EPA compliance.

We further decreased the cathode potential to -0.60 V (20 ℃) or -0.50 V (80 ℃) and conducted SeDER via a six-electron pathway. Note that the cathodic potential for both pathways was determined by LSV scan prior to the long-term experiment. At 20 ℃, the Se concentration dropped continuously from 6.83 to 4.46 mg L^{-1} over the 6-h experiment (Fig. 4A), with an average Se removal rate of 56.48 mg m^{-2} h^{-1}, a total removal efficiency of 34.7%, and a Faradaic efficiency of 5.5%. A large portion of generated red Se(0) was suspended in the solution (Fig. S5). Increasing the solution temperature to 80 ℃ resulted in an elevated Se removal rate of 89.29 mg h^{-1} m^{-2}, a higher removal efficiency of 50.1%, and a more desirable Faradaic efficiency of 9.0% (Fig. 4B). We also identified crystalline grey Se(0) at the bottom of the cell (Fig. S6). An over 50% removal in 6 hours suggests that the six-electron pathway was kinetically favorable compared to the four-electron pathway, though we could not perform an accurate kinetic analysis due to a failure to separate the Se(IV)/Se(-II) peak from the hydrogen evolution reaction peak at pH 5.5 in both LSV and rotating disk electrode tests (Fig. S7 and S9). A previous kinetic study confirmed that six-electron pathway is also controlled by mass transport, and the standard rate constant of Se(IV)/Se(-II) is three orders of magnitude higher than Se(IV)/Se(0) at pH 2.[32]

Eventually, we extended the operation time of six-electron SeDER to 24 hours for maximum Se removal under 80 ℃ (Fig. 4C). We started with 0.1 mM Se (6.79 mg L^{-1}) to simulate a typical Se concentration in FGD wastewater, achieving a 6-h, 12-h, and 24-h removal efficiency of 55.6%, 79.2%, and 94.5%, respectively. Under 0.01 mM (0.78 mg L^{-1}) and 0.001 mM Se (79.05 μg L^{-1}), SeDER is a more mass-transfer constrained process and achieved slightly lower 24-h removal efficiencies (87-89%), compared to that of 0.1 mM Se(IV). Based on our results, SeDER could serve as bulk removal and polishing processes to manage diluted Se water streams. It

demonstrated the capability to meet EPA ELG daily maximum (23 μg L^{-1}, 18-h operation) and monthly average discharging standards (12 μg L^{-1}, 22-h operation), based on the linear fit under 0.001 mM (R^2= 0.98, Fig. 4C). Se(VI) was not reduced over 24-h of operation with an electrode potential of -0.5V at 80 ℃ (left panel, Fig. 4D). We observed 6.9 mg L^{-1} Se removal in both Se(IV) and Se(IV)+Se(VI) experimental groups (middle and right panels, Fig. 4D), with comparable Faradaic efficiency of ~6.6%. Hence, the presence of Se(VI) in aqueous solution is not expected to interfere with electrochemical Se(VI) reduction by occupying reaction sites or competing for electrons.

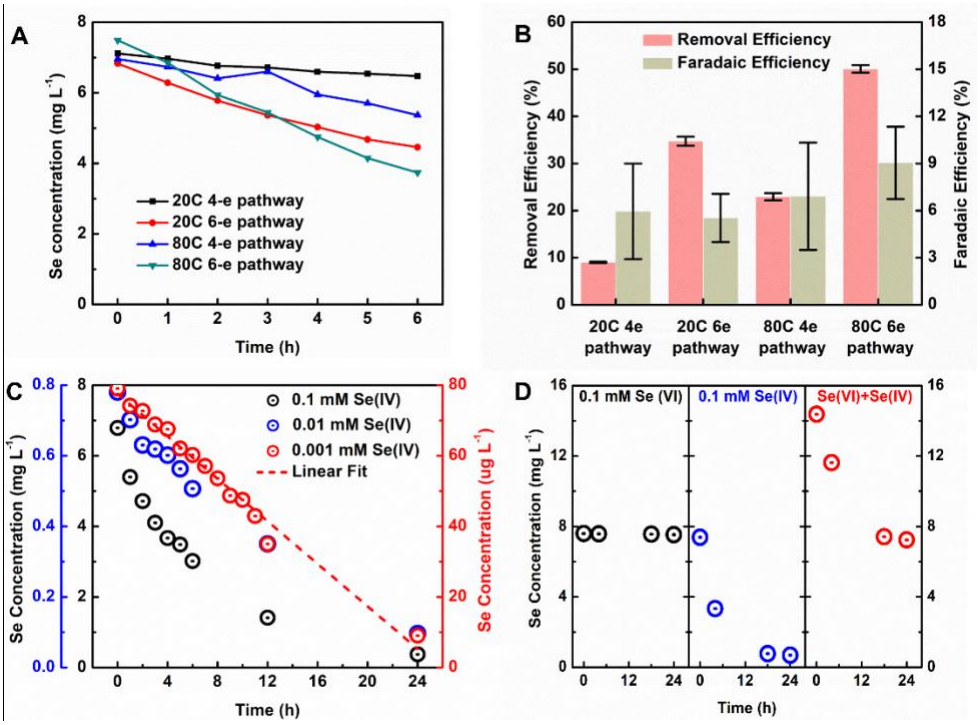

Figure 4. Electrochemical Se(IV) reduction regarding (A) soluble Se concentration profile in 6-hour operations with 0.1 mM Se(IV), (B) removal and Faradaic efficiencies for 6-hour operations with 0.1 mM Se(IV), (C) soluble Se concentration profile in 24-hour operations under 80 ℃ with 0.001 mM, 0.01 mM, and 0.1 mM Se(IV), and (D) Se reduction performance in 0.1 mM Se(VI),

0.1 mM Se(IV), and 0.1 mM Se(VI) + 0.1 mM Se(IV) mixture under a six-electron pathway at 80 °C.

Perspectives and implications. Our results demonstrated the potential of SeDER to effectively remove Se(IV) in weakly acidic solutions via four- and six-electron pathways. This study also encourages substantial research toward improving the Se removal rate and Faradaic efficiency in SeDER via optimized reactor design, electrode selection, and operational modes.

One major challenge for SeDER application in dilute wastewater or natural water treatment is the slow electrochemical reduction of Se(VI) oxyanions. Immobilizing metallic catalysts on the cathode surface could potentially facilitate Se(VI) reduction to Se(-II). For example, previous studies have utilized underpotentially deposited copper (Cu) or Cadmium (Cd) on Au to reduce Se(VI) to metal selenide (Se(-II)), followed by an anodic stripping of Cu or Cd to collect elemental Se on the electrode surface.[46, 47] However, this approach is limited by the amount of pre-deposited Cu or Cd on the substrate surface and requires periodic regeneration of Cu or Cd layer. On the other hand, Se(VI)/Se(0) reduction pathway would bury the surface-coated metallic catalyst within the Se layer. To sustain continuous Se(VI) reduction, Se(VI)/Se(IV) conversion is more desirable than Se(VI)/Se(0) or Se(VI)/Se(-II) pathways, followed by a separate step/process for Se(IV) removal. One example may be to strategically reverse the polarity of electrode once the initial step of Se(VI)/Se(IV) conversion is complete, resulting in Se(0) deposition on the opposite electrode in the following step. This strategy has been used in the electrochemically mediated reduction of Cr(VI) to Cr(III) in previous studies.[29, 48] Alternatively, a solution-phase metallic or biological catalyst could be used to address Se(VI)/Se(IV) conversion,[38] but this approach would require

careful catalyst design to precisely stop reduction at the Se(IV) phase, instead of further reducing to Se(0). Meanwhile, an *in-situ* or downstream separation process (e.g., membrane filtration) will be required to retain the solution phase catalyst within the electrochemical cell, thereby minimizing potential health and ecological concerns associated with discharging the catalyst.

Generation of crystalline Se(0) could be a key solution to tackle the surface-limited four-electron SeDER process. However, maintaining a high wastewater temperature between 50-80 °C would be relatively challenging if onsite SeDER is not immediately available. Direct heating of wastewater would render SeDER energetically and economically less competitive, considering the relatively high heat capacity of water. Hence, we need to develop localized heating strategies to control the formation of the Se(0) phase. One potential strategy is to resistively heat the cathode to ensure a desirable surface temperature (70-80°C) and facilitate the deposition of crystalline Se(0). However, considering a low heat conductivity of elemental Se (10^{-3} W cm^{-1} K^{-1}), continuous deposition of crystalline Se could hinder efficient heat transfer to the outermost surface layer, resulting in the formation of amorphous Se and termination of SeDER. Hence, better electrode or system design needs to be coupled with localized heating to sustain SeDER at low temperatures.

A comprehensive understanding of potential parasitic reactions in complex water matrices will also be essential to evaluating the technoeconomic feasibility of SeDER. Industrial and agricultural wastewaters contain many oxyanions (e.g., sulfate, nitrate, nitrite, phosphate, and metal oxyanions) that may compete with SeDER for electrons and lower the Faradaic efficiency of SeDER. On the other hand, the presence of metal cations (such as copper) may lead to co-deposition with Se, which could enhance the overall Se removal performance by increasing the

conductivity of the deposited layer. These phenomena could significantly affect the SeDER process design and will require a thorough evaluation.

Finally, while Au cathode and Pt anode provide stable and reusable interfaces for electrochemical reactions, alternative electrode materials may reduce the capital cost of the SeDER system. Carbon-based or iron-based cathodes are the most promising candidates and should be comprehensively examined for both the four- and six-electron SeDER pathways. Meanwhile, anode selection and design are equally important to the SeDER process. A Ti counter electrode (1×5×0.125 cm) could offer us comparable Se removal efficiency to Pt electrode in a 6-h operation (Fig. S10). However, the long-term operation would result in gradual oxidation of Ti to TiO_2, along with an obvious color change (Fig. S11) and a high overpotential for oxygen evolution reaction.

Supporting Information

Detailed information of three-electrode system setup, electrode cleaning protocol, quantification of performance metrics, images of the electrochemical cell and electrode surface after four- and six-electron pathways, kinetic analysis of SeDER can be found in the Supporting Information.

Corresponding Author

Meagan S. Mauter. Phone: (650) 725-4911; e-mail: mauter@stanford.edu

Notes

The authors declare no competing financial interest.

Acknowledgments

This work was partially supported by a faculty startup fund of Stanford University. Shiqiang Zou was financially supported by the National Science Foundation (DMR-2023833). We sincerely thank Dr. Alexander V. Dudchenko for his help with the customized 3-D printed lids.

REFERENCES

(1) Holmes, A. B.; Gu, F. X., Emerging nanomaterials for the application of selenium removal for wastewater treatment. *Environ. Sci. Nano* **2016,** *3*, (5), 982-996, DOI 10.1039/C6EN00144K.
(2) Winkel, L. H. E.; Johnson, C. A.; Lenz, M.; Grundl, T.; Leupin, O. X.; Amini, M.; Charlet, L., Environmental Selenium Research: From Microscopic Processes to Global Understanding. *Environ. Sci. Technol.* **2012,** *46*, (2), 571-579, DOI 10.1021/es203434d.
(3) Rayman, M. P., The importance of selenium to human health. *Lancet* **2000,** *356*, (9225), 233-241, DOI 10.1016/S0140-6736(00)02490-9.
(4) Gingerich, D. B.; Grol, E.; Mauter, M. S., Fundamental challenges and engineering opportunities in flue gas desulfurization wastewater treatment at coal fired power plants. *Environ. Sci. Water Res. Technol.* **2018,** *4*, (7), 909-925, DOI 10.1039/C8EW00264A.
(5) Santos, S.; Ungureanu, G.; Boaventura, R.; Botelho, C., Selenium contaminated waters: an overview of analytical methods, treatment options and recent advances in sorption methods. *Sci. Total Environ.* **2015,** *521*, 246-260, DOI 10.1016/j.scitotenv.2015.03.107.
(6) Tan, L. C.; Nancharaiah, Y. V.; van Hullebusch, E. D.; Lens, P. N. L., Selenium: environmental significance, pollution, and biological treatment technologies. *Biotechnol. Adv.* **2016,** *34*, (5), 886-907, DOI 10.1016/j.biotechadv.2016.05.005.
(7) Twidwell, L.; McCloskey, J.; Joyce, H.; Dahlgren, E.; Hadden, A. Removal of selenium oxyanions from mine waters utilizing elemental iron and galvanically coupled metals. Proceedings of the Jan D. Mill Symposium—Innovations in Natural Resource Processing, Salt Lake City, UT, USA, 2005; 299-313.
(8) Holmes, A. B.; Khan, D.; de Oliveira Livera, D.; Gu, F., Enhanced photocatalytic selectivity of noble metallized TiO2 nanoparticles for the reduction of selenate in water: tunable Se reduction product H2Se(g)vs. Se(s). *Environ. Sci. Nano* **2020,** *7*, (6), 1841-1852, DOI 10.1039/D0EN00048E.
(9) Ohlendorf, H. M.; Santolo, G. M.; Byron, E. R.; Eisert, M. A., Kesterson Reservoir: 30 Years of Selenium Risk Assessment and Management. *Integr. Environ. Assess. Manag.* **2020,** *16*, (2), 257-268, DOI 10.1002/ieam.4222.
(10) He, Y.; Xiang, Y.; Zhou, Y.; Yang, Y.; Zhang, J.; Huang, H.; Shang, C.; Luo, L.; Gao, J.; Tang, L., Selenium contamination, consequences and remediation techniques in water and soils: a review. *Environ. Res.* **2018,** *164*, 288-301, DOI 10.1016/j.envres.2018.02.037.
(11) U. S. EPA. Aquatic Life Ambient Water Quality Criterion for Selenium - Freshwater 2016, Office of Water, Washington, D.C., 2016.
(12) U.S. EPA. National primary drinking water regulations: Long Term 1 Enhanced Surface Water Treatment Rule (final rule). Federal register 67.9 (2002): 1811.
(13) Kuroda, M.; Yamashita, M.; Miwa, E.; Imao, K.; Fujimoto, N.; Ono, H.; Nagano, K.; Sei, K.; Ike, M., Molecular cloning and characterization of the srdBCA operon, encoding the respiratory selenate reductase complex, from the selenate-reducing bacterium Bacillus selenatarsenatis SF-1. *J. Bacteriol. Res.* **2011,** *193*, (9), 2141-2148, DOI 10.1128/JB.01197-10.
(14) Ridley, H.; Watts, C. A.; Richardson, D. J.; Butler, C. S., Resolution of Distinct Membrane-Bound Enzymes from *Enterobacter cloacae* SLD1a-1 That Are Responsible for Selective Reduction of Nitrate and Selenate Oxyanions. *Appl. Environ. Microbiol.* **2006,** *72*, (8), 5173-5180, DOI 10.1128/AEM.00568-06.

(15) Nancharaiah, Y. V.; Lens, P., Ecology and biotechnology of selenium-respiring bacteria. *Microbiol. Mol. Biol. Rev.* **2015,** *79*, (1), 61-80, DOI 10.1128/MMBR.00037-14.
(16) Sonstegard, J.; Pickett, T.; Harwood, J.; Johnson, D., Full scale operation of GE ABMet® biological technology for the removal of selenium from FGD wastewaters. *International Water Conference* **2007,** *68*, 580-585.
(17) U.S. EPA. Effluent Limitations Guidelines and Standards for the Steam Electric Power Generating Point Source Category (proposed rule). Federal Register: Washington, D.C., 2019.
(18) Hamilton, S. J., Review of selenium toxicity in the aquatic food chain. *Sci. Total Environ.* **2004,** *326*, (1-3), 1-31, DOI 10.1016/j.scitotenv.2004.01.019.
(19) LeBlanc, K. L.; Wallschläger, D., Production and Release of Selenomethionine and Related Organic Selenium Species by Microorganisms in Natural and Industrial Waters. *Environ. Sci. Technol.* **2016,** *50*, (12), 6164-6171, DOI 10.1021/acs.est.5b05315.
(20) Li, M.; Farmen, L. M.; Chan, C. K., Selenium Removal from Sulfate-Containing Groundwater Using Granular Layered Double Hydroxide Materials. *Ind. Eng. Chem. Res.* **2017,** *56*, (9), 2458-2465, DOI 10.1021/acs.iecr.6b04461.
(21) Hu, C.; Chen, Q.; Chen, G.; Liu, H.; Qu, J., Removal of Se(IV) and Se(VI) from drinking water by coagulation. *Sep. Purif. Technol.* **2015,** *142*, 65-70, DOI 10.1016/j.seppur.2014.12.028.
(22) Gui, M.; Papp, J. K.; Colburn, A. S.; Meeks, N. D.; Weaver, B.; Wilf, I.; Bhattacharyya, D., Engineered iron/iron oxide functionalized membranes for selenium and other toxic metal removal from power plant scrubber water. *J. Membr. Sci.* **2015,** *488*, 79-91, DOI 10.1016/j.memsci.2015.03.089.
(23) Ling, L.; Pan, B.; Zhang, W.-x., Removal of selenium from water with nanoscale zero-valent iron: mechanisms of intraparticle reduction of Se (IV). *Water Res.* **2015,** *71*, 274-281, DOI 10.1016/j.watres.2015.01.002.
(24) Staicu, L. C.; Morin-Crini, N.; Crini, G., Desulfurization: Critical step towards enhanced selenium removal from industrial effluents. *Chemosphere* **2017,** *172*, 111-119, DOI 10.1016/j.chemosphere.2016.12.132.
(25) Chen, R.; Sheehan, T.; Ng, J. L.; Brucks, M.; Su, X., Capacitive deionization and electrosorption for heavy metal removal. *Environ. Sci. Water Res. Technol.* **2020,** *6*, (2), 258-282, DOI 10.1039/C9EW00945K.
(26) Baek, K.; Kasem, N.; Ciblak, A.; Vesper, D.; Padilla, I.; Alshawabkeh, A. N., Electrochemical removal of selenate from aqueous solutions. *Chem. Eng. J.* **2013,** *215*, 678-684, DOI 10.1016/j.cej.2012.09.135.
(27) Jia, R.; Wang, Y.; Wang, C.; Ling, Y.; Yu, Y.; Zhang, B., Boosting Selective Nitrate Electroreduction to Ammonium by Constructing Oxygen Vacancies in TiO2. *ACS Catal.* **2020,** *10*, (6), 3533-3540, DOI 10.1021/acscatal.9b05260.
(28) Rodriguez-Valadez, F.; Ortiz-Éxiga, C.; Ibanez, J. G.; Alatorre-Ordaz, A.; Gutierrez-Granados, S., Electroreduction of Cr(VI) to Cr(III) on Reticulated Vitreous Carbon Electrodes in a Parallel-Plate Reactor with Recirculation. *Environ. Sci. Technol.* **2005,** *39*, (6), 1875-1879, DOI 10.1021/es049091g.
(29) Su, X.; Kushima, A.; Halliday, C.; Zhou, J.; Li, J.; Hatton, T. A., Electrochemically-mediated selective capture of heavy metal chromium and arsenic oxyanions from water. *Nat. Commun.* **2018,** *9*, (1), 4701, DOI 10.1038/s41467-018-07159-0.

(30) Alekperov, A., Electrochemistry of selenium and tellurium. *Russ. Chem. Rev.* **1974,** *43*, (4), 235, DOI 10.1070/RC1974v043n04ABEH001803.
(31) Andrews, R. W.; Johnson, D. C., Voltammetric deposition and stripping of selenium (IV) at a rotating gold-disk electrode in 0.1 M perchloric acid. *Anal. Biochem.* **1975,** *47*, (2), 294-299, DOI 10.1021/ac60352a005.
(32) Maranowski, B.; Strawski, M.; Osowiecki, W.; Szklarczyk, M., Study of selenium electrodeposition at gold electrode by voltammetric and rotating disc electrode techniques. *J. Electroanal. Chem.* **2015,** *752*, 54-59, DOI 10.1016/j.jelechem.2015.05.037.
(33) Wang, Y.; Xue, Y.; Su, J.; Zheng, S.; Lei, H.; Cai, W.; Jin, W., Efficient electrochemical recovery of dilute selenium by cyclone electrowinning. *Hydrometallurgy* **2018,** *179*, 232-237, DOI 10.1016/j.hydromet.2018.05.019.
(34) Guarneros-Aguilar, C.; Calzadilla, O.; Baron-Miranda, J.; Fernandez-Muñoz, J.; Caballero-Briones, F., Phase control in selenium electrodeposition with bath temperature and deposition potential. *Mater. Res. Express* **2019,** *6*, (6), 066412, DOI 10.1088/2053-1591/ab0875.
(35) Cordoba, P.; Staicu, L. C., Flue gas desulfurization effluents: An unexploited selenium resource. *Fuel* **2018,** *223*, 268-276, DOI 10.1016/j.fuel.2018.03.052.
(36) Gao, S.; Tanji, K.; Peters, D.; Herbel, M., Water selenium speciation and sediment fractionation in a California flow-through wetland system. *J. Environ. Qual.* **2000,** *29*, (4), 1275-1283, DOI 10.2134/jeq2000.00472425002900040034x.
(37) Maslennikov, A.; Peretroukhine, V.; David, F.; Lecomte, M. *Selenium electrochemistry. Applications in the nuclear fuel cycle*; Paris-11 Univ.: 1999.
(38) Hageman, S. P. W.; van der Weijden, R. D.; Weijma, J.; Buisman, C. J. N., Microbiological selenate to selenite conversion for selenium removal. *Water Res.* **2013,** *47*, (7), 2118-2128, DOI 10.1016/j.watres.2013.01.012.
(39) Von Hippel, A.; Bloom, M., The electroplating of metallic selenium. *J. Chem. Phys.* **1950,** *18*, (9), 1243-1251, DOI 10.1063/1.1747918.
(40) Saji, V. S.; Lee, C.-W., Selenium electrochemistry. *RSC Adv.* **2013,** *3*, (26), 10058-10077, DOI 10.1039/C3RA40678D.
(41) Lister, T. E.; Stickney, J. L., Atomic Level Studies of Selenium Electrodeposition on Gold(111) and Gold(110). *J. Phys. Chem.* **1996,** *100*, (50), 19568-19576, DOI 10.1021/jp9621540.
(42) Kotkata, M. F.; Kandil, K. M., A study of the electrical conductivity of amorphous-crystalline selenium mixtures. *Mater. Sci. Eng.* **1987,** *95*, 287-293, DOI 10.1016/0025-5416(87)90521-0.
(43) Yu, J.; Lu, J.; Kang, Y., Removal of sulfate from wet FGD wastewater by co-precipitation with calcium hydroxide and sodium aluminate. *Water Sci. Technol.* **2018,** *77*, (5), 1336-1345, DOI 10.2166/wst.2018.019.
(44) Lizell, B., The Electrical Conductivity of Liquid Selenium and Selenium-Tellurium Mixtures. *J. Chem. Phys.* **1952,** *20*, (4), 672-676, DOI 10.1063/1.1700514.
(45) Su, J.; Lin, X.; Zheng, S.; Ning, R.; Lou, W.; Jin, W., Mass transport-enhanced electrodeposition for the efficient recovery of copper and selenium from sulfuric acid solution. *Sep. Purif. Technol.* **2017,** *182*, 160-165, DOI 10.1016/j.seppur.2017.03.056.

(46) Strobl, J. R.; Scherson, D. A., Communication—The Reduction of Selenate Mediated by Underpotential Deposited Copper on Gold Electrodes in Acidic Solutions: Analytical Applications. *J. Electrochem. Soc.* **2016,** *163*, (13), H1066, DOI 10.1149/2.0241613jes.
(47) Han, Q.; Strobl, J.; Scherson, D., Communication—Selenate Reduction Induced by Cadmium Underpotential Deposition on Gold in an Aqueous Acidic Electrolyte. *J. Electrochem. Soc.* **2019,** *166*, (8), H283, DOI 10.1149/2.0461908jes.
(48) Kim, K.; Cotty, S.; Elbert, J.; Chen, R.; Hou, C. H.; Su, X., Asymmetric Redox-Polymer Interfaces for Electrochemical Reactive Separations: Synergistic Capture and Conversion of Arsenic. *Adv. Mater.* **2020,** *32*, (6), 1906877, DOI 10.1002/adma.201906877.